a longitudinal apparent attraction, although the type of motion produced by this attraction is rather different. Hence we find that under certain conditions the center of gravity of the spacecraft "attracts" all the particles in the cabin, in the sense that the particles have a tendency to be brought together here. (In the case of $-35° < \alpha < +35°$, there is instead an apparent repulsion by the center of gravity of the cabin.)

Because the spacecraft is assumed to have a negligible mass, one may ask why its center of gravity has such a remarkable property. The answer is that this point merely defines the state of motion of the whole assembly. Suppose that the mass of the spacecraft is much smaller than the mass of the particles and that their original common center of gravity were situated at an r larger than the center of gravity of the spacecraft. Then the particles would move more slowly than the spacecraft and would hit its backside wall, with the result that the spacecraft would be displaced outward so that its center of gravity would (almost) coincide with the center of gravity of the particles. (An exact statement is possible only if the original state of motion of the particles is known.)

The apparent attraction is more important than the Newtonian attraction between the bodies of mass m_1 under the condition

$$\mathbf{f}_a \gg \frac{\kappa m_1}{\rho^2} \tag{23}$$

which means that

$$\frac{\rho}{r_0} \gg \left(\frac{m_1}{M_c}\right)^{1/3} \tag{24}$$

For a spacecraft in orbit ($r_0 = 10^9$ cm) around the earth ($M_c = 6 \times 10^{27}$ g), particles with a mass of 6 g should be much more than 1 cm apart.

5) *Application to astrophysical problems.* I have treated a very simple model in order to clarify some aspects of celestial mechanics that have not attracted much attention so far. It is important to consider the extent to which similar phenomena may occur in astrophysics. The role of the spacecraft walls in our model is to compel all particles to orbit with the same period. However, this effect could also be achieved by other means, for example, by viscous effects, mutual collisions, and electromagnetic effects. There is a certain analogy between the lining up in the cabin of the particles, which originally are in random positions and have random velocities and the formation of jet streams of meteoroids or asteroids (*2*). The perturbation-produced focusing of these particles may be related to the formation of comets [see (*3*)].

It is also possible that my model may be applicable to some galactic phenomena. The general concentration of matter in the galactic plane is, of course, somewhat related to the phenomena I have studied, but it is possible that my model is also applicable to phenomena on a smaller scale. For example, the apparent attraction may keep a nebula together or make it contract even if the self-gravitation is insufficient for this contraction.

HANNES ALFVÉN
Department of Applied Physics and Information Science, University of California, San Diego, La Jolla 92037

References

1. H. Alfvén, *Nature* **225**, 229 (1970); ——— and G. Arrhenius, *Astrophys. Space Sci.* **8**, 338 (1970).
2. L. Danielsson, in *Physical Studies of the Minor Planets*, T. Gehrels, Ed. (*Proceedings of the 12th Colloquium of the International Astronomical Union*, Tucson, Ariz., March 1971, in press); J. Trulsen, *ibid.*
3. J. Trulsen, in *Proceedings of the International Astronomical Union Symposium on the Motion, Evolution of Orbits, and Origin of Comets*, Leningrad, August 1970, in press; H. Alfvén, in *ibid.*

26 April 1971

Rapidly Changing Radio Images

Abstract. *Differences in total transit time can give rise to images that expand at arbitrarily high speed. Two versions of a model based on this idea can account for the varying microwave structure reported for the quasar 3C 279. Other possible examples are suggested.*

Very-long-baseline interferometry is beginning to enable investigators to probe the spatial structure of the energetic cores of extragalactic sources, on the scale of light years. Since many of these sources are known to vary appreciably in microwave output over times of the order of 1 year, interpretation of the source structure will require full attention to retardation effects. It was pointed out a long time ago (*1, 2*) how these effects can give rise to kinematic illusions, that is, images (at arbitrary distance) whose apparent rate of change can far exceed c, the speed of light, even though no actual particle or signal velocity does so.

Recent measurements (*3*) suggest that such effects might be occurring in the quasar 3C 279; at a radio wavelength of 3.8 cm a fine structure is detected below 1×10^{-3} arc sec which shows definite changes over a 4-month interval. Because of the incomplete sampling, the interferometric pattern cannot yet be uniquely transformed into a spatial picture, but the simplest picture in accord with the measurements consists of two well-separated moving spots. The fluxes of the two spots are equal to better than 5 percent, and the spots move apart at a rate which—if the source is at the cosmological red-shift distance—is several times the speed of light.

The equal flux of the two moving spots in 3C 279 suggests that they are associated with a single physical source. Motivated by these findings, we present two versions of a kinematic model for rapidly moving double images associated with a single source (*4*). Observations of such patterns would not be surprising in any object that is variable over the time required for light to traverse the diameter, regardless of whether or not 3C 279 turns out to be a clear-cut example.

Model 1. Suppose an explosive event within the quasar sends out a sudden burst of energy in all directions, in the form of relativistic particles or of electromagnetic or other waves. Suppose further that a sharp increase in the radiation emitted at the observation frequency takes place when the primary pulse reaches a sphere of radius R, and that the increased emission is confined to a narrow shell (Fig. 1).

Under these conditions all parts of the shell brighten simultaneously; however, a distant observer receives the signal from each part at a different time, depending on its distance. Let $t = 0$ denote the instant when the brightening of the forward point A is first detected; then point B is seen to flare up at time

$$t = R(1 - \cos\theta)/c \tag{1}$$

At first, the brightened region is a disk of diameter

$$D(t) = 2\,(2Rct - c^2t^2)^{1/2} \tag{2}$$

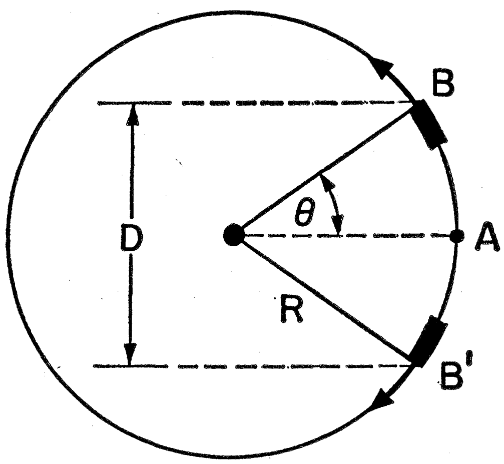

Fig. 1. Diagram showing how differences in transit time can lead to rapid image expansion. For model 1 a primary burst emitted at the center causes all parts of the screen to brighten simultaneously. The image observed at time t consists of the two spots whose edges are at B, B'. The apparent diameter is given by Eq. 2.

[See (*1*) for details.] The apparent expansion velocity of the disk,

$$\frac{dD}{dt} = 2^{1/2} c \left(\frac{R}{ct}\right)^{1/2} \left(1 - \frac{ct}{R}\right) \left(1 - \frac{ct}{2R}\right)^{-1/2} \quad (3)$$

is infinite at $t = 0$ and remains much greater than c for times that are short relative to R/c. If the persistence time τ is finite, then for $t > \tau$, the image becomes a ring whose outer diameter is given by Eq. 2 and whose inner diameter is $D(t - \tau)$.

If the initiating burst, instead of being emitted in all directions, is confined to a plane, an observer located in that plane sees, for $t > \tau$, two spots which separate along a fixed line in the plane of the sky. The separation between the leading edges of the spots is given by Eq. 2. The apparent width of each spot,

$$W(t) = \tfrac{1}{2}\,[D(t) - D(t - \tau)] \quad (4)$$

is a maximum at $t = \tau$ when the spots have just formed, and then diminishes steadily. The fluxes from the two components are always equal, provided that the initiating pulse and the conditions in the shell are sufficiently isotropic in azimuth. (The directional properties of the radiation pattern do not affect the relative intensity since the components are always observed symmetrically.)

Within the context of the model outlined here, the observation of the two spotlike sources strongly suggests that the initiating event is concentrated in a plane (*5*). A natural way to define such a preferred plane is through rotation. The general picture that emerges is consistent with the hypothesis that the primary source for the phenomenon is a rotating condensed object—a spinar (*6*).

Model 2. For a rotating source, another model that leads to similar kinematic effects assumes a local enhancement of activity, confined to a small angular sector, that radiates energy (electromagnetic, hydromagnetic, or corpuscular) in the form of a beacon. When the beacon impinges on a distant spherical "screen" (Fig. 2), it initiates a radiative process at the observation frequency with a short lifetime τ. Provided that the phase relations are sufficiently well maintained, the active "spot" sweeps the screen at a speed ΩR, where $\Omega R/c$ can be arbitrarily high (Ω is the angular velocity of the beacon). For a while the "source" runs ahead of the signal. The first signal received by the observer comes from point P^* where the component of source velocity in the direction of the observer is just c, that is,

$$\cos\phi^* = c/\Omega R \quad (5)$$

(Angles are now being measured from the transverse diameter.) Afterward, the observer receives signals from points both ahead of and behind P^*. After a time τ, P^* is no longer visible and the image divides into two spots, one running forward and one running backward along the screen. The latter spot is, in a sense, observed propagating backward in time. This "optical boom" is analogous to a fully supersonic boom.

The angle ϕ (see Fig. 2) associated with the leading edge of the spot observed at time t is given implicitly by the relation

$$\Omega t = (\Omega R/c)(\sin\phi^* - \sin\phi) + (\phi - \phi^*) \quad (6)$$

Equation 6 has two solutions, one for the forward-moving spot, $\phi_f > \phi^*$ and one for the backward-moving spot, $\phi_b < \phi^*$; the apparent velocities of the two images are given by

$$v_{f,b} = \frac{-\Omega R \sin\phi_{f,b}}{1 - \frac{\Omega R}{c}\cos\phi_{f,b}} \quad (7)$$

and the apparent separation

$$D = R(\cos\phi_f - \cos\phi_b)$$

can be written in the form

$$D = Rc\left(\frac{1}{v_b} - \frac{1}{v_f}\right) \quad (8)$$

[for $(v/c)^2 \gg 1$]. The apparent width of each spot is given by an expression analogous to Eq. 4. The initial expansion velocity is infinite, as in model 1, and the images are at first symmetric with respect to P^*; a first-order expansion for short times gives

$$\frac{v_{f,b}}{c} = \mp\left[1 - \left(\frac{c}{\Omega R}\right)^2\right]^{1/4} \left(\frac{R}{2ct}\right)^{1/2} \quad (9)$$

(see also Eq. 3.) After a while an asymmetry develops, which depends on the parameter $\Omega R/c$. When $\Omega R/c$ approaches infinity, ϕ^* approaches $\pi/2$, and the images are symmetric at all times. The model in this limit becomes formally identical to model 1, as it must since now the beacon sweeps the screen infinitely fast. The fluxes from the two spots are again equal, provided there is sufficient azimuthal symmetry and the initiating beacon does not change appreciably while it sweeps through the angle $\phi_f - \phi_b$; in the asymmetric case, there is the additional requirement that the radiation pattern be sufficiently isotropic.

Both of our models involve a preferred plane, but it is hardly likely that the observer is situated just in that plane. In the more general case in which the line of sight makes an angle α with that plane, the observed image is modified by projection, but the main effect persists. The apparent separation and expansion velocity are, as before, given by Eqs. 2 and 3 (model 1), and Eqs. 7 and 8 (model 2), with R replaced by $R/\cos\alpha$. A new effect is that, although the position angle of the images remains constant, their centroid moves in the plane of the sky (Fig. 3). If the screen is not spherical, an asymmetry develops in model 1 as well, and the position angle changes with time (Fig. 4). There is in this case an additional time delay that depends on the speed of the initiating pulse, but this delay causes no significant changes in the results.

The time dependence of the measured flux is similar in the two models: it increases until $t = \tau$, when the individual spots form. Thereafter, the flux is proportional to the fraction of the radiating screen under observation at the time. This fraction decreases steadily, but more slowly than the width of the spots; thus the image might exhibit a limb-brightening effect at the edge of the screen. There is, however, an additional decline in flux due to the directionality of the radiation pattern; if the screen emission is strongly beamed in the radial direction, the limb brightening will be overcome; the images then disappear much sooner than they would on purely kinematic grounds. The kinematic disappearance time is $R/(c \cos \alpha)$ in model 1 (*7*), and nearly the same in model 2 unless $\Omega R/c$ is close to unity.

Model 2 predicts that the entire process will repeat with a period

$$T = 2\pi/\Omega$$

provided that the disturbance that gives rise to it persists for longer than one period. Observation of such periodicity would constitute strong evidence in favor of this picture. If the period is less than the disappearance time, it is, in principle, possible to observe two or more recurrences simultaneously.

A possible physical realization of the "screen" we have postulated is the stagnation surface for the flow of plasma from the center of activity. The required short persistence time can be plausibly obtained if the observed emission is synchrotron radiation. A transverse magnetic field of the order of 1 gauss would make the radiative lifetime a few months for electrons emitting at ~ 10 Ghz. A field of such magnitude, decreasing as $1/r$ over distances of tens of light years, is quite plausible for spinar models. The magnetic energy required is $\sim 10^{57}$ to $\sim 10^{58}$ ergs, a modest amount on the scale of quasar energies.

It is helpful to express the theoretical results in terms of the directly observed angular separation ψ between the components. By definition, D of Eq. 2 is equal to $L\psi$, where L is the "angular size distance" to the source. (The cosmological model enters only in the determination of L from the red shift, the Hubble constant, and q_0.)

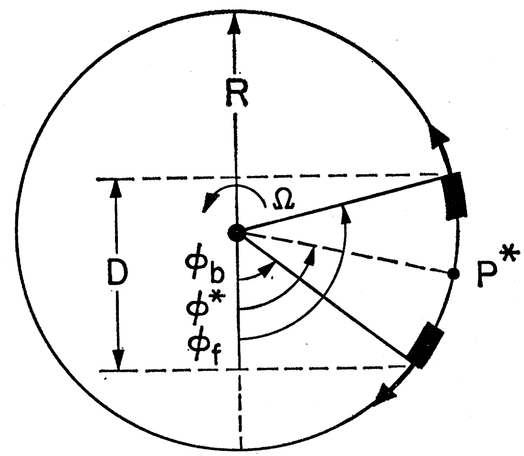

Fig. 2. Kinematics for model 2. A beacon from the rotating primary source sweeps the screen at a formal speed of ΩR. The first signal detected by the observer comes from point P^*. After some time he sees two spots traveling in opposite directions as shown by the arrows. The apparent speed of separation is given by Eq. 7.

If ψ and $\dot\psi$ are specified, the parameters of model 1 are uniquely determined from Eqs. 2 and 3. For $ct \ll R$ (which turns out to be justified for the 3C 279 data), one obtains:

$$\frac{R}{\cos \alpha} = \frac{L^2}{4c}\psi\dot\psi \qquad (10)$$

$$t = \tfrac{1}{2}\, \psi/\dot\psi \qquad (11)$$

The factor $\frac{1}{2}$ in Eq. 11 is a consequence of the $t^{1/2}$ dependence of $\psi(t)$ for short times; this behavior is an intrinsic feature of the model (see the appendix). Notice that t is independent of L and therefore of all cosmological effects. The results are little different for model 2 as long as ct is $\ll R$.

In the idealized model, the edges of the spots are perfectly sharp, and ψ in Eq. 11 clearly refers to the separation between the leading edges. The quantities determined by observation are the angular separation between the centers of intensity of the spots, say, ψ_c, its rate of change $\dot\psi_c$, and an effective angular width for each spot, δ. In terms of these quantities, Eq. 11 reads

$$t = \tfrac{1}{2}\, (\psi_c/\dot\psi_c)\ (1 + \delta/\psi_c)/(1 + \dot\delta/\dot\psi) \qquad (12)$$

In our models, δ is negative, and, when the spots are well separated, Eq. 13 satisfies (see the appendix)

$$\dot\delta/\dot\psi = -\,\delta/\psi \qquad (13)$$

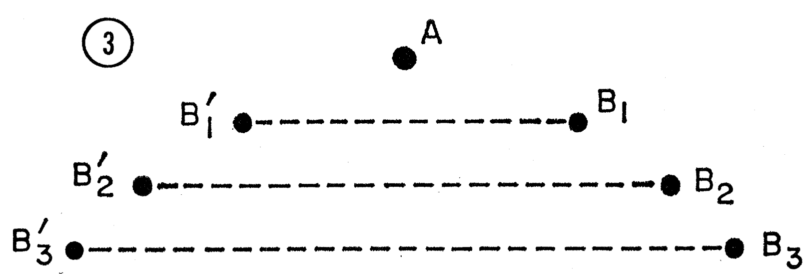

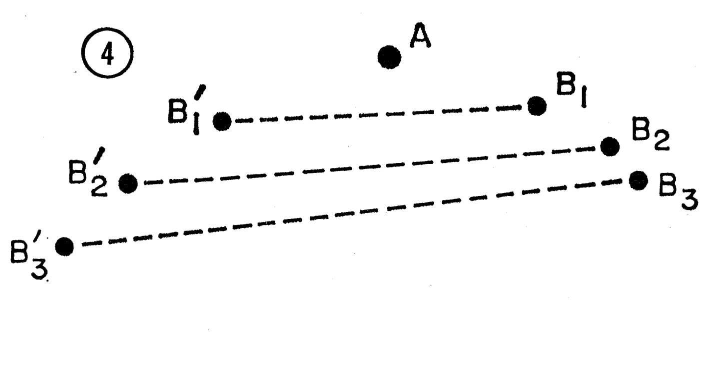

Fig. 3 (top). Sequence of images expected when the observer is not in the preferred emission plane. The position angle between the spots remains constant, but their centroid moves. Fig. 4 (bottom). Sequence of images expected when the screen is not perfectly spherical (model 1). The position angle changes with time. In model 2, such an asymmetry develops after a long time even for a spherical screen.

For small values of δ/ψ, Eq. 12 becomes

$$t \approx \tfrac{1}{2}\, \frac{\psi_c}{\dot{\psi}_c}\left(1 + \frac{2\delta}{\psi_c}\right) \qquad (14)$$

which can be evaluated from measurable quantities. Within the same approximations, $\psi\dot{\psi}$ is constant across the spot, so that $\psi_c\dot{\psi}_c$ can be substituted in Eq. 10 with no corrections.

For 3C 279, the observed results are as follows (*3*): $\psi_c = 1.55 \pm 0.05 \times 10^{-3}$ arc sec (October 1970); $\dot{\psi}_c = 1.2 \pm 0.3 \times 10^{-6}$ arc sec per day (October 1970 through February 1971). The quoted value of $\dot{\psi}_c$ is for that fit which assumes a simple radial expansion. As for the width, we are informed (*8*) that, although a finite width gives a fit that is clearly better than that of point sources, the data do not yet specify δ. We therefore take, somewhat arbitrarily, $\psi/\delta \approx 5 \pm 2$. If our model applies to these observations, the indicated values of the parameters are then: $t = 2.5 \pm 0.8$ years; $R/\cos\alpha = 36 \pm 9$ light years (for $L = 3 \times 10^9$ light years, corresponding to a red shift $z = 0.54$, $q_0 = 1$). The angle θ subtended at the primary source by the images presently observed is about 20°; since τ depends directly on δ, it is very poorly determined, but is of the order of 1 year.

The total flux from 3C 279 is known to exhibit complicated time variations. Measurements at 3.75 cm (*9*) indicate what appear to be two overlapping outbursts with peaks around 1967.0 and 1968.3, and rise times under 1 year; thereafter, the flux diminished steadily. The date for the onset of the phenomenon calculated from our model, 1968.3 ± 0.8, is consistent, within the rather large uncertainty, with the second of these outbursts. In view of the ambiguities associated with an interpretation of the interferometric data, as well as in the choice of the flux associated with the event in question against a varying background, we do not consider the comparison of dates to be particularly significant. Indeed, a simple linear extrapolation based on the present separation speed gives no worse agreement. A sharper test of the model, in our view, is provided by its definite prediction of a slowdown in the expansion rate. Such a slowdown should be observable before long, if our model applies.

Among other objects in which effects similar to the ones discussed here are liable to occur, a prime candidate is 3C 345, a quasar in which strong indications of periodicity are provided by optical observations (*10*). With an apparent period of about a year and outbursts observed to persist over three or four periods, there would seem to be a good chance to observe multiple microwave images in this quasar.

Similar phenomena can be expected also in galactic objects. For example, it is tempting to speculate whether the wisp phenomena in the Crab Nebula and the observed variations in microwave emission (*11*) can be related to model 2. The period in this case is known to be much shorter than the disappearance time for the spots if R is at the wisp distance, $\sim 10^{17}$ cm. If a change in pulsar activity occurs on a time scale of weeks or less, one might expect to observe a train of overlapping spots, with an advancing edge.

It is also attractive to consider in this light the pattern of the radio sources near Sco X-1 (*12*). There the lateral, weak sources (at a distance of $\sim 10^{17}$ cm if they are at all associated with the x-ray source) are relatively steady, but the central source exhibits flares and sudden variations which—if taken at face value—imply exceedingly rapid spatial changes. Further measurements are badly needed, to search for the much postulated, but still elusive, rotational nature of the energy source for this object.

Appendix

It is worth while to point out the mathematical structure of this family of models. Let the generalized coordinate s define the points from which the observed emission emanates, and let $t(s)$ be the total travel time for signals reaching us from the point s. The point first observed is determined by the extremum condition

$$dt/ds = 0 \qquad \text{(I)}$$

Let s^* be the value of s that satisfies Eq. I, and let $t(s^*) = t_0$. Then, provided that the function $t(s)$ is regular, we can expand in the vicinity of s^* and put

$$t(s) - t_0 \approx \tfrac{1}{2}\left(\frac{d^2t}{ds^2}\right)_{s=s^*}(s - s^*)^2 \quad \text{(II)}$$

The quadratic equation (Eq. II) has two solutions, s_f and s_b, which describe the two images observed. Let $\psi(s)$ be the angle between the lines of sight to s and s^*; the rate at which this angle increases is given by

$$\frac{d\psi}{dt} = \psi'(s)\,\frac{ds_{f,b}}{dt} \qquad \text{(III)}$$

which is infinite at $t = t_0$ by virtue of Eq. I. Furthermore, in the neighborhood of s^*,

$$\frac{d\psi}{dt}\Big|_{f,b} \approx$$

$$\pm\, 2^{1/2}\,\psi'(s^*)\left(\frac{d^2t}{ds^2}\right)_{s=s^*}(t - t_0)^{-1/2} \quad \text{(IV)}$$

The $t^{-1/2}$ behavior of the expansion rate is seen to be an intrinsic feature of this class of models, provided that $t(s)$ is regular and its second derivative does not vanish.

The angular size of the spot is

$$\delta = \tfrac{1}{2}\,[\psi(t) - \psi(t - \tau)]$$

For t appreciably larger than τ, one has

$$\delta \approx \tfrac{1}{2}\,\frac{d\psi}{dt}\,\tau \propto \frac{\tau}{(t - t_0)^{1/2}} \qquad \text{(V)}$$

which is proportional to ψ^{-1}.

A. CAVALIERE
American Science and Engineering, Cambridge, Massachusetts 02142
P. MORRISON
L. SARTORI
Massachusetts Institute of Technology, Cambridge 02139

References and Notes

1. P. Morrison and L. Sartori, *Phys. Rev. Lett.* **16**, 414 (1966); *Astrophys. J.* **152**, L139 (1968); *ibid.* **158**, 541 (1969) (footnote *2* gives a detailed history of the effect and its applications, which date back to Nova Persei in 1901).
2. M. J. Rees, *Nature* **211**, 468 (1966); *Mon. Notic. Roy. Astron. Soc.* **135**, 345 (1967); *Astrophys. J.* **152**, L145 (1968).
3. C. A. Knight, D. S. Robertson, A. E. E. Rogers, I. I. Shapiro, A. R. Whitney, T. A. Clark, R. M. Goldstein, G. E. Marandino, N. R. Vandenberg, *Science* **172**, 52 (1971); A. R. Whitney, I. I. Shapiro, A. E. E. Rogers, D. S. Robertson, C. A. Knight, T. A. Clark, R. M. Goldstein, G. E. Marandino, N. R. Vandenberg, *ibid.* **173**, 225 (1971).
4. The idea of model 1 was expressed by T. Gold in discussions at the Rumford Symposium, Brookline, Mass., April 1971.
5. An image consisting of two points results also if the initiating pulse is omnidirectional but the enhanced emission is restricted to a one-dimensional (pencil-shaped) region. Such a model seems less plausible on physical grounds.
6. P. Morrison, *Astrophys. J.* **157**, L73 (1969); A. Cavaliere, P. Morrison, F. Pacini, *ibid.* **162**, L133 (1970), and references therein.
7. Theoretically, the images would begin to converge again after reaching the edge of the screen, as radiation from the backward hemisphere is observed. Detection of such an effect would require a considerable emission in the backward direction, which seems hardly likely.
8. I. I. Shapiro, personal communication.
9. W. A. Dent, personal communication; H. D. Aller, *Astrophys. J.* **161**, 1 (1970).
10. T. D. Kinman, E. Lamla, T. Ciurla, E. Harlan, C. A. Wirtanen, *Astrophys. J.* **152**, 357 (1968).
11. G. T. Wrixon, J. R. Gott, A. A. Penzias, *ibid.* **165**, 23 (1971).
12. R. M. Hjellming and C. M. Wade, *ibid.* **164**, L1 (1971).
13. We are most grateful to Dr. I. I. Shapiro for providing us with interferometric results in advance of publication, and for illuminating discussions of their interpretation. We also thank Dr. W. A. Dent and Dr. R. M. Hjellming for communication of unpublished data. Work done at M.I.T. was supported in part by NASA grant NGL-22-009-019 and in part by NSF grant GP-11453.

18 May 1971